

EDGE DETECTION TECHNIQUE FOR SIMULTANEOUS MEASUREMENT OF TOTAL SUSPENDED SOLIDS AND TURBIDITY

*Rijal Hakiki¹, Yuniati Zevi¹, Barti Setiani Muntalif¹ and Irwan Purnama²

¹Department Environmental Engineering, Bandung Institute of Technology, Indonesia; ²National Research and Innovation Agency (BRIN), Indonesia

*Corresponding Author, Received: 02 July 2023, Revised: 13 Sep. 2023, Accepted: 17 Sep. 2023

ABSTRACT: APHA Standard methods 2130B and 2540D have proven valid and reliable methods to determine turbidity and total suspended solids (TSS). However, both methods have drawbacks and limitations. Carcinogenicity of formazin, inconsistency in preparation, and interference are the primary concerns in turbidity measurement. Equipment complexity, working steps, and measurement time are primary concerns in TSS measurement. The edge detection technique (EDT) is an alternative to overcome the drawbacks and limitations. This research aims to conduct the performance test of the proposed method using pro-analytical grade kaolin (Sigma-Aldrich K7375), which has non-toxic properties compared to the formazin standard. Natural water samples from three different sampling locations became another subject in the EDT-based measurement method performance test. Steps included are elemental characterization with SEM-EDS-JEOL-JSM6510LA and particle size analysis with zeta sizer Horiba SZ-100. Turbidity measurement with Eutech TN100 and the TSS measurement with the gravimetric approach. Counted particle (CP) measurement through the EDT compared with the standard measurement. It showed that kaolin characteristics are closer to the natural suspension indicated by the more identical elemental compositions than the formazin elemental characteristics. Another result showed a correlation between kaolin concentration (KC), turbidity level, TSS concentration, and the counted particle is > 0.9 . The proposed approach showed promising results indicated by the % Relative Standard Deviation $< 20\%$ for KC 0.5-20 mg/L and $< 40\%$ for KC 40-100 mg/L, in the linear range of 0.5-100 mg/L. Using a sample cell with a flat surface may improve the performance of the proposed approach. It is thus possible to reduce the reflection of light, which is a noise source in the measurement result.

Keywords: Kaolin, Turbidity, Suspended Solids, Edge Detection, Image Processing

1. INTRODUCTION

Suspended solids indicate water quality that correlates with the level of contamination of microorganisms, organic matter, and sediment formation in the waters [1], [2]. Turbidity is another water quality parameter that can describe the amount of suspended solids in the water [3]. The relation between suspended solids concentration and turbidity is known to be influenced by the colour of the solution, density, shape, and size of the particles [4]. To anticipate interference that may occur, several types of alternative measurement techniques have been developed [5]. The sequential multi-parameter analysis is available on the HACH DR1900, Lovibond MD 100, and photoLab 6600 portable instruments. These analytical instruments involve a test kit of reagents and specific wavelengths for each parameter, except for TSS and turbidity parameters, which do not require adding particular chemicals. The specific wavelength selection aims to obtain the maximum detection response that underlies the measurement selectivity [6]. In commercial meters, a beam of light is

converted into an electrical signal using an electronic photo-detector. It is then amplified and visualized as a specific value through the stage of mathematical substitution [7].

In addition to using electronic photo-detectors, image-processing techniques are an alternative approach to measuring and monitoring suspended particle concentrations in water. Satellite image processing is an option that can be used to determine the spatial profile of turbidity and suspended sediment concentrations in waters [8], [9]. Correlating the grayscale intensity with turbidity is one of the image processing approaches performed [10], [11]. This study aims to determine the performance level of the edge detection technique in the simultaneous analysis of turbidity and TSS levels in artificial and natural water samples. Kaolin is a potential alternative for turbidity standards [12] due to the carcinogenic properties of formazin [13] and inconsistencies in its preparation [14]. Other considerations include the elemental characteristics and particle size of the kaolin suspension, which are closer to those naturally suspended in natural water samples. Edge

detection technique as an approach to measure TSS and turbidity levels through digital image processing. Compared to existing turbidity [14] and TSS [15] measurements, substituting the CP value into the linear regression equation allows the simultaneous determination of turbidity level and TSS concentration.

2. MATERIALS AND METHODS

Pro-analytical grade kaolin (Sigma-Aldrich K7375) is the primary material for preparing various concentrations of standard series. The two-megapixel CMOS camera uses a custom light-isolation chamber to isolate the images from the ambient light interferences (Fig.1).

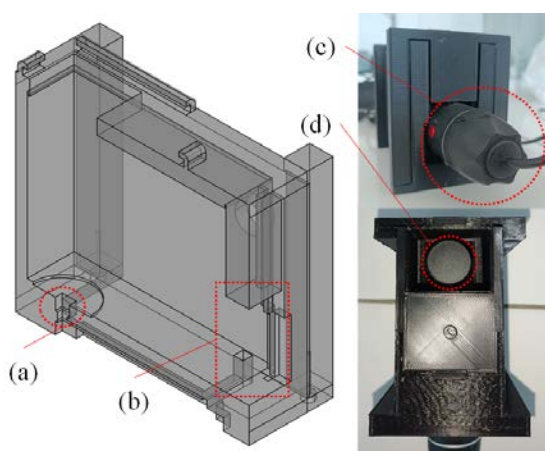


Fig.1 Configuration of the custom light-isolation chamber, (a) Light source (LED-SMD5050) position on the sectional-3D model of measurement chamber (MC), (b) Camera holder, (c) Camera position on the printed MC, and (d) Sample cell position on the printed MC

The custom chamber has a standalone SMD5050-LED light source at 90° to the camera sensor. It uses a ± 3.2 Volt standalone power supply to light up the SMD5050-LED. The dimension of the custom light-isolation chamber is 100 (L) x 72 (W) x 90 (H) mm. The enclosure is made of polylactic acid (PLA) filament and printed with the Creality CR-10 Mini 3D printer. The suspension was placed in the HANNA HI 731331 sample cell.

2.1 Suspended Particle Characterizations

Elemental characteristics and particle size are the related physical characteristics of the sample suspension. Determination of elemental characteristics of the dried suspension samples using a JEOL JSM-6510 LA scanning electron microscope-energy dispersive X-ray spectrometer (SEM-EDS). The vacuum drying process at room temperature was carried out on suspension of formazin 4000 NTU (HACH 246149) and surface

water samples, except for the kaolin sample, which is already in powder form. Particle size analysis of the suspended solids using a zeta sizer Horiba SZ-100. The investigation was conducted directly on the 40 NTU formazin suspension and surface water samples. For the sample of the kaolin suspension, the stage of dispersion in distilled water with a concentration of 40 mg/L is necessary. Fig. 2 shows an image of a dried sample of formazin, a natural sample and kaolin powder.

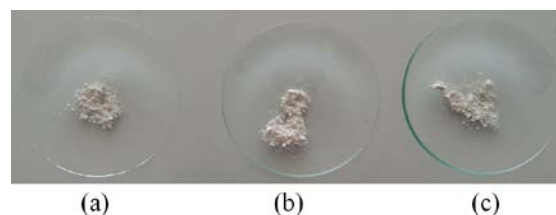


Fig.2 Dried sample of (a) Formazin, (b) Kaolin powder, and a dried sample of (c) Natural sample

2.2 Suspended Kaolin Preparations

Kaolin concentration was varied in the range of 0.5-100 mg/L to determine the effect of kaolin concentration (KC) on the counted particle (CP), TSS, and turbidity. The kaolin concentration range has been determined based on initial trial results, which show that the maximum observed kaolin suspension is 100 mg/L. The boundary between suspended particles with the dispersant is not observable above this concentration. Sample prepared by dispersing pro-analytical grade kaolin in distilled water at concentrations of 0.5, 5, 20, 40, 70, 90, and 100 mg/L. Each concentration of kaolin dispersion was stirred for 5 minutes with a magnetic stirrer at a medium stirring speed to minimize bias in the preparation step. The turbidity level was measured using a commercially available turbidimeter, the Eutech TN100. The analysis of the TSS concentration for each concentration of the kaolin suspension followed the standard APHA 2540D method, which includes a vacuum filtration process and gravimetric principles in the measurement stage.

2.3 Sampling of Natural Water Sample

The samples were taken from the Cilemahabang River in the Bekasi district in West Java, Indonesia. It was taken randomly at three different locations (Fig. 3) at coordinates -6.284009, 107.170071 (sampling point A); -6.283775, 107.170266 (sampling point B); -6.276109, 107.177954 (sampling point C). The sampling point chosen considers the anthropogenic activities that exist at the locations. The sampling points were located in the Jababeka Industrial Estate, classified as an integrated industrial, commercial and residential

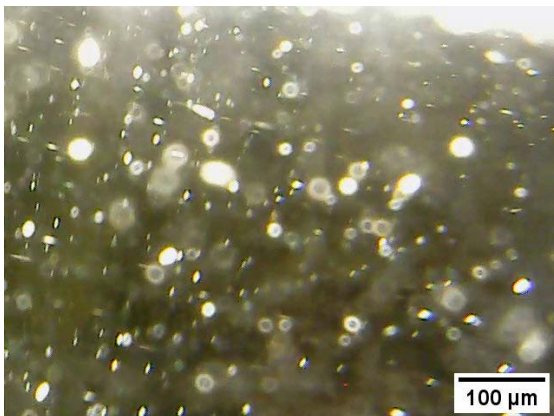
area. It may represent the heterogeneity of anthropogenic activities as the influential factor of water quality [16].



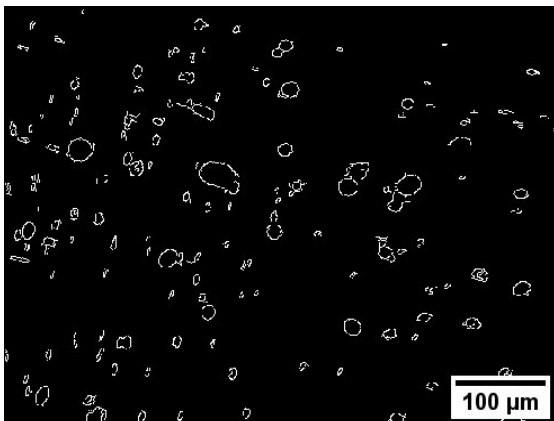
Fig.3 Sampling points of natural water sample

2.4 Edge Detection Technique

The edge detection technique consists of several stages: image frame acquisition, RGB to grayscale (8-bit) image conversion, contrast adjustment, threshold setting, and object counting process [17].



(a)



(b)

Fig.4 Captured frame image (a) Before processing and (b) After processing

The image acquisition process involves the use of

plugable digital viewer v3.1.07 software. As for the other stages using ImageJ 1.53t, a public domain open source software [18]. The 100 frames of images were captured at a resolution of 1920 x 1080 pixels for 1 minute to obtain representative quality and quantity for further processing (Fig.4). The default contrast setting was chosen at the image processing stage, considering the sufficient contrast level between the object and the background. The thresholds for the image frame for kaolin and natural water suspension samples are a minimum of 231 and a maximum of 255. The particle counting process uses the particle analysis feature of the ImageJ software [19]. Repeatability calculations, range, and linearity determinations are several methods to assess the proposed measurement method's performance. The performance tests were performed on the data from six repeated readings of the kaolin suspension at different concentrations in the range of 0.5 to 100 mg/L.

3. RESULTS AND DISCUSSION

Measurement results and data analysis presented include a discussion of suspended particle characteristics and the influence of KC on turbidity, TSS, and CP. Furthermore, this section presents the performance test of the EDT and its implementation on natural water samples.

3.1 Suspended Particle Characteristics

The use of high-purity kaolin (Sigma-Aldrich K7375) was based on the results of SEM-EDS analysis, which showed that the elemental composition of kaolin was closer to the composition of natural water samples, as presented in Table 1.

Table 1 Elemental composition of formazin, kaolin, and natural suspended particle

Element	% Mass		
	Natural	Formazin	Kaolin
C	10.5	67.0	NA
O	52.4	24.2	59.0
Mg	0.9	0.3	NA
Al	9.0	1.2	19.9
Si	19.9	4.4	21.2
Ca	3.9	2.9	NA
Fe	3.4	NA	NA
Total	100.0	100.0	100.0

The mass percentage of oxygen (O), aluminium (Al), and silicon (Si) are the dominant elements contained in the surface water (52.37% O, 8.98% Al, and 19.87% Si), and kaolin suspension solution (58.96% O, 8.98% Al and 19.87% Si).

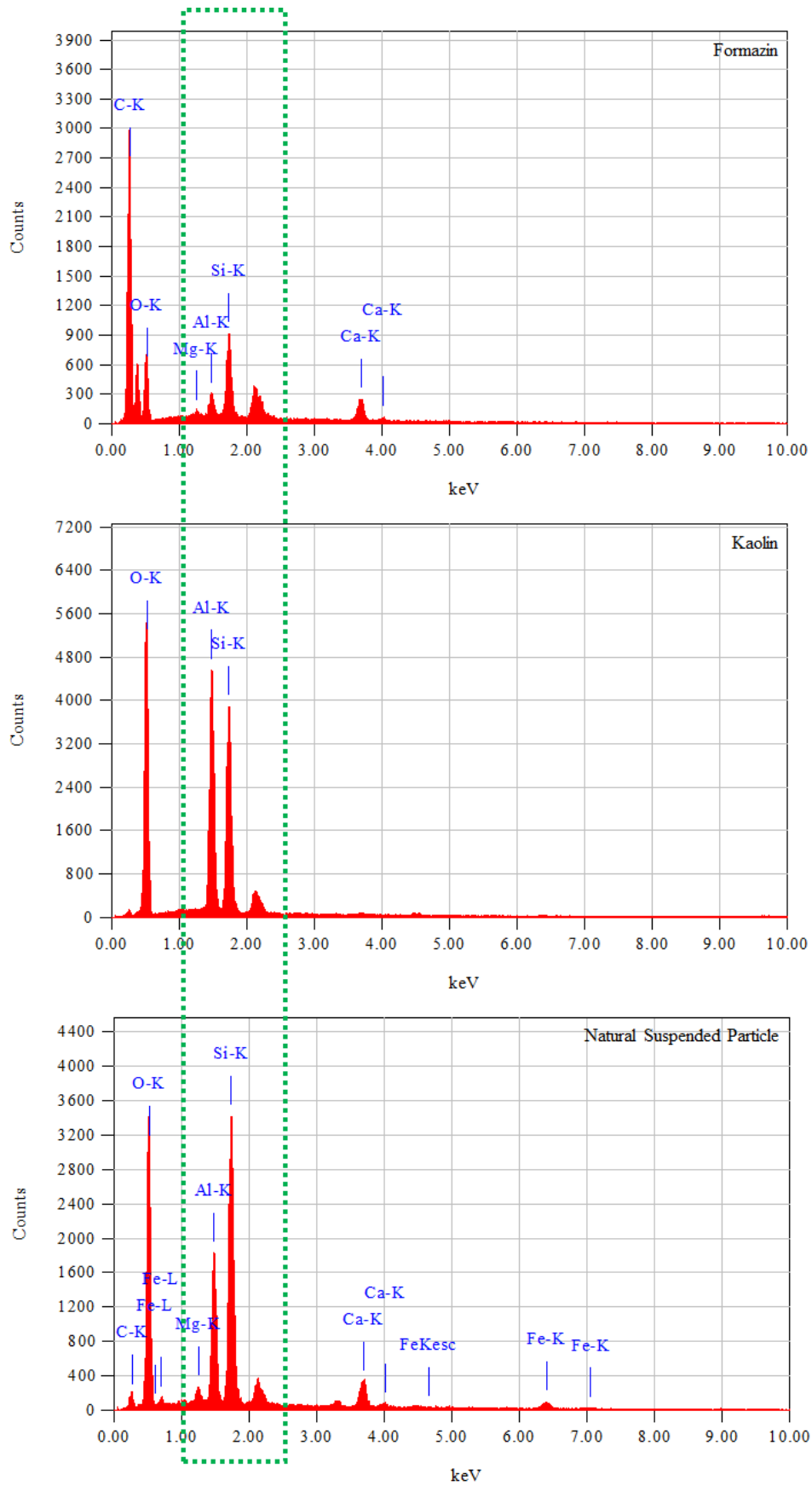


Fig.5 Elemental characteristics of formazin, kaolin, and natural suspended particle

Whereas in the formazin suspension solution, the mass percentage of carbon (C), oxygen (O), and silicon (Si) are the dominant elements detected respectively at 67% C, 24.17% O and 4.38% Si of the total elemental content in each of the characterized solutions. Visual comparison amongst the suspended particle composition strengthened the fact that the elemental composition of kaolin was closer to the composition of natural water samples, as presented in Fig.5.

With a much lower silicon mass percentage than the other two types of suspension, in the wavelength range of 300-1200 nm, the particle range that includes the Mie scattering area, which is the basis for developing the nephelometric measurement method, is between 0.01-100 μm [14]. Clay, silt, and sand particles, the dominant turbidity (Si) components, are in this size range. Particle size analysis with the zeta sizer shows that the suspended particle size is within the size range according to the Mie scattering theory, as presented in Table 2.

Table 2 Particle size of formazin, kaolin, and natural suspended particle

Sample	Particle Size-Zeta (μm)	Particle Size-EDT (pixel ²)
Formazin	2.18	57.76
Kaolin	4.65	175.95
Natural Suspended Particle	3.44	125.71

Although the sizes of the three types of suspended particles are within the Mi scattering range area, considering their elemental composition. Formazin is considered a less representative turbidity standard for determining the level of water clarity.

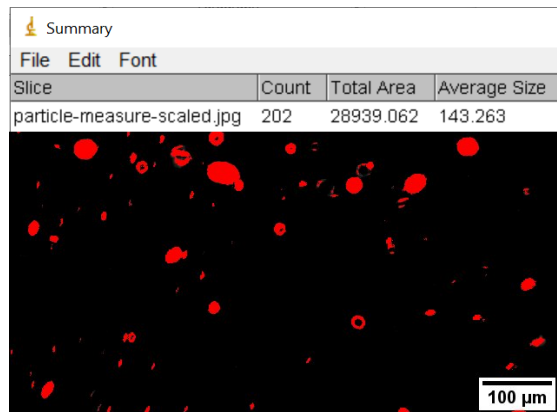


Fig.6 Particle size measurement with ImageJ

The particle size provided in Table 2 is the average value from some repetitive measurements. Heterogeneity in particle size of natural suspension is closer to the kaolin suspension than the formazin.

Fig.6 shows manual processing in particle size measurement of suspended particles. The custom macro script is used with ImageJ to process multi-frame images.

3.2 Influence of Kaolin Concentration on Turbidity, TSS, and Counted Particle

The results of laboratory experiments showed that changes in the mass of dispersed kaolin affected the number of measured particles. As shown in Fig.7, the same applies to the turbidity and TSS. The plot of KC against CP, turbidity, and TSS resulted in a coefficient of determination (*R-square*) of 0.8825, 0.9991, and 0.9092, respectively. The results indicate a reasonably good deterministic pattern between the four variables that are the focus of discussion in this study. Regression results confirm the deterministic pattern, which shows a *P-value* of 1.7811E-05 (KC against CP), 6.39804E-15 (KC against Turbidity), and 5.50945E-06 (KC against TSS). All the *P-values* are lower than alpha in a confidence level of 95%, which shows the dependency of turbidity, TSS and CP on the kaolin concentration.

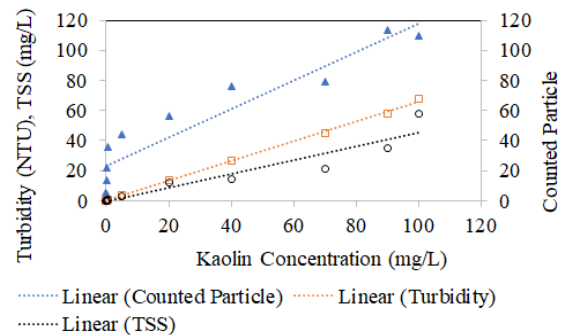


Fig.7 Relation between kaolin concentration, turbidity, TSS, and counted particle

The linear equations resulting from Fig.7 can explain the influence of kaolin concentration (KC) against the measured turbidity, TSS and the counted particles (CP). Equations (1), (2), and (3) represent deterministic patterns for counted particles, turbidity, and TSS, respectively.

$$y = 0.9458x + 22.877 \tag{1}$$

$$y = 0.6565x + 0.1571 \tag{2}$$

$$y = 0.4558x - 0.2867 \tag{3}$$

As shown in Table 3, substituting kaolin concentration into the linear equation resulted in a higher CP than measured. In contrast to turbidity and TSS, the substitution results in lower values than measured. However, using the substitution results directly as a basis for prediction is

impossible. It only shows the relation and the existence of deterministic patterns amongst the focus parameters. Further performance tests are necessary to determine the proposed approach's potential implementation in measurements and monitoring activities.

Table 3 Measurement results (Mea.) and substitution results (Sub.) of kaolin concentration into the Equations (1), (2), and (3)

Kaolin (mg/L)	Counted Particle (Avg)		Turbidity (NTU)		TSS (mg/L)	
	Sub.	Mea.	Sub.	Mea.	Sub.	Mea.
0.0	27.7	5.1	0.2	0.0	-0.3	0.0
0.5	56.5	35.5	0.5	0.5	-0.0	0.6
5.0	64.7	44.2	2.7	3.8	0.9	2.7
20.0	76.4	56.6	9.3	13.9	5.2	12.0
40.0	95.1	76.3	17.4	26.3	6.4	14.7
70.0	97.5	78.9	29.8	45.1	9.4	21.3
90.0	130.1	113.4	38.2	57.9	15.8	35.3
100.0	126.5	109.6	44.5	67.6	26.2	58.0

3.3 The Performance of Edge Detection Technique

The EDT performance test assesses the developed turbidity and TSS measurement methods. Fig.8 displays a plot of kaolin concentration (KC) against counted particles (CP). The random Brownian motion of suspended particles affects the scatter pattern of the light beam [20]. The closer the density number of both constituents, the more dispersion of particles and the more random movement in a suspension system. It is possible that the same phenomena also occurred in the commercial turbidity meter measurement but cannot be observed visually.

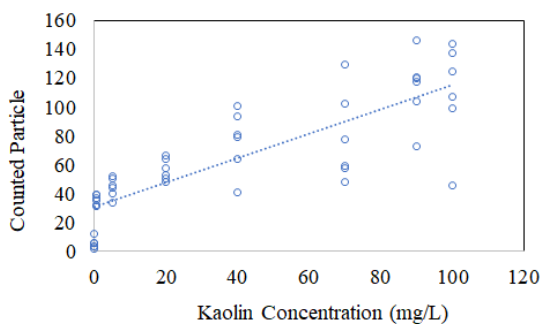


Fig.8 The six repetitions of counted particle (EDT-based) measurements

Considering this phenomenon, a one-time measurement result with a commercial turbidity meter does not mean a one-time sample reading. It involves averaging multi-reading results and shows the single number of turbidity shown on the meter screen. The commercial turbidity meter does not

measure turbidity directly. It predicts turbidity based on the light-scattering intensity recorded by the photo-detector [20]. The same applies to the EDT approach. The final turbidity number is not measured directly. It resulted from the mathematical substitution of the counted particle (CP) as the surrogate parameter of turbidity. The counted particle (CP) measurement results in each replicate out of six replicate readings show a poor deterministic pattern but still show a significant dependency of CP to KP, as indicated by the coefficient of determination (*R-square*) 0.7436 with a *P-value* of 7.89121E-13 in a confidence level of 95%. However, the *R-square* alone cannot directly indicate EDT performance. Testing for repeatability, linearity, and range are additional criteria that can indicate EDT performance [21], [22]. The repeatability of measurements is expressed as per cent relative standard deviation (%RSD), as presented in Table 4.

Table 4 Percentage of relative standard deviation from six repetitive measurements of CP in the linear range

Kaolin Concentration (KC) (mg/L)	CV Horwitz (%)	RSD (%)
0.5	17.76	9.90
5	12.56	15.03
20	10.19	12.90
40	9.18	28.26
70	8.44	39.79
90	8.13	21.20
100	8.00	32.76

The best linearity could be achieved in the KC range of 0.5 mg/L - 100 mg/L, as indicated by a correlation coefficient (*r*) of 0.97 for the CP to KC plot, 0.97 for CP to turbidity plot, and 0.91 for CP to TSS plot. However, this value is still lower than the required linearity acceptance with $r > 0.99$ [23]. The %RSD at various KC are higher than the Horwitz CV values, except at the KC of 0.5 mg/L. Referring to APVMA (2004) [23] states that the level of acceptability of repeatability is at a %RSD value $\leq 20\%$, only at KC of 0.5 mg/L - 20 mg/L that meets the acceptability criteria. The performance test results determine the concentration range chosen for the regression equation. It will be a basis for estimating KC, turbidity level, and TSS concentration. The plot of CP against turbidity, TSS, and KC is presented in Fig.9.

The zero KC equals zero NTU and zero TSS concentration in mg/L. In contrast to the CP, zero KC is not equal to zero CP due to the reflection of light in the image, which causes noise. [24]. Light reflection was affected by the rounded surface of the

cylindrical sample cell used in this experiment. Similar phenomena may occur considering the same cylindrical sample cell used in commercial turbidity meter. Background corrections may be required to overcome these conditions, including using a non-rounded sample cell and adjusting the light source position and normalization.

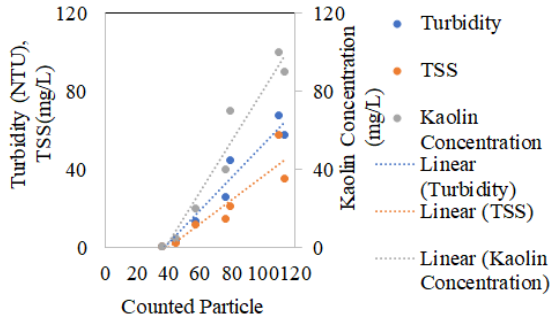


Fig.9 Relation between CP, kaolin concentration, turbidity, and TSS

The best prediction results are close to the measured values obtained from the linear regression, as stated in Equations (4), (5), and (6).

$$y = 1.3022x - 49.244 \quad (4)$$

$$y = 0.8523x - 31.933 \quad (5)$$

$$y = 0.608x - 24.044 \quad (6)$$

With R -square = 0.9463, Equation (4) can predict the kaolin concentration (KC) based on the CP. It is possible to predict turbidity levels based on the CP using Equation (5), yielding an R -square of 0.9439. It is possible to use Eq. (6) to predict TSS concentrations based on CP, with an R -square of 0.8336. The predictive ability strengthened by the P -value for all regression is lower than alpha in a confidence level of 95%. P -values related to Equations (4), (5), and (6) are 0.0018, 0.0020, and 0.0158.

The minimum CP, which is substitutable in linear Equations (4), (5), and (6), is 40, with the highest CP value being 115. The lowest CP value is determined based on the smallest positive value obtained from the substitution results. In comparison, the highest value is determined based on the highest concentration of kaolin (100 mg/L). The substitution results showed that the CP range of 40-115 was equivalent to the KC range of 2.84-100.51 mg/L, the turbidity range of 2.16-66.08 NTU, and the TSS range of 0.28-45.88 mg/L.

3.4 Implementation of EDT on Natural Water Sample

The measured counted particle (CP) of the three

natural water samples is 59-71. With measured turbidity levels in the range of 21.07-25.88 NTU and TSS concentrations in the 13.40-19.60 mg/L range. Substitution of CP into Equation (4) yielded KC values of 43.21 mg/L (sample A), 34.09 (sample B), and 27.58 (sample C). Table 5 presents the measurement results of turbidity, Total Suspended Solids (TSS), and Counted Particles (CP) in the three natural water samples. Turbidity number and CP consistently follow the TSS concentration pattern.

Table 5 Measurement results of CP, turbidity, and TSS for three natural water samples

Sample	Counted Particle	Turbidity (NTU)	TSS (mg/L)
A	71	25.88	19.60
B	64	24.52	15.80
C	59	21.07	13.40

Theoretically, turbidity may represent suspended solids concentration. Nevertheless, as observed in Table 5, there are some differences in the measured number. For the same sample, turbidity shows higher values than the TSS due to the interaction between the monochromatic light beam and the photosensitive materials suspended or dissolved in the sample. [25].

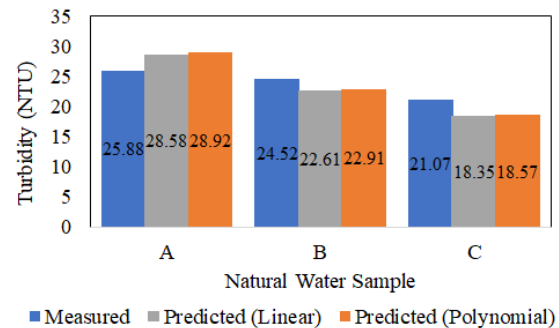


Fig.10 Comparison between measured and predicted turbidity level

The suspended particles are the main target to quantify in turbidity measurement, not the dissolved materials. The presence of dissolved photosensitive substances is unavoidable in natural water samples. Based on the multi-variable plots shown in Fig.9, there were only slight differences between the linear correlation coefficient and the second-order polynomial regression coefficient—comparison of CP replacement values in linear and polynomial regression models to find the best-fitting regression model. The closeness of the substitution results is the main criterion for determining the best regression equation. Comparison of substitution results CP into the linear Equation (5) and CP into the second-order polynomial regression equation is

shown in Fig.10. The predicted turbidity level from the two equations appears similar for each natural water sample. Unlike the TSS concentration, the substitution results of CP into the linear equation (6) produce a TSS concentration closer to the TSS concentration measured gravimetrically. Based on these results, the linear regression equation provides a better prediction closer to the measured concentration. Fig.11 compares the substitution results for CP in the linear Equation (6) and CP in the second-order polynomial regression equation.

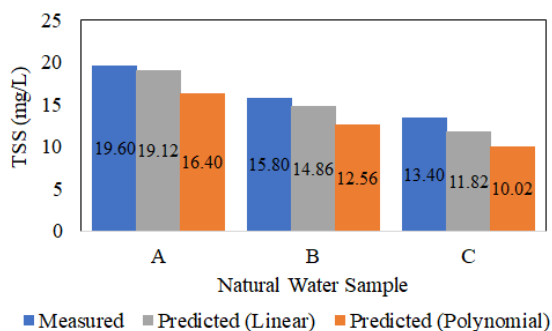


Fig.11 Comparison between measured and predicted TSS concentration

4. CONCLUSIONS

The standard measurement method is not the most perfect approach for measuring turbidity and TSS. Each developed method has its approach basis and limitation. As a part of image processing techniques, edge detection techniques can be an alternative approach to the existing standard methods. The measurement principles rely on substituting counted particles into the produced linear regression equations. It has the potential for further implementation as a basis for simultaneous measurements of turbidity and TSS. The range of 40 to 115 is the lower and upper limits of the developed measurement method. It may measure samples with low to medium-range turbidity and TSS. The dilution step would be necessary for the sample with a higher turbidity level before being measured with the EDT. The noise caused by the shape of the sample cell and the limited measurement range are some issues related to the proposed approach. Another noise cause possibly resulted from the camera's ability to capture the image. The delay time in the image acquisition process should be set to allow the suspended particle to be slow enough to be captured by the camera. The faster movement of the suspended particles results in a blurry image, which makes it harder for further processing. Improving the camera specification (faster camera detection) and the usage of the flat surface sample cell are recommended to overcome the noise. The better camera specification not only overcomes noise

problems but also possibly improves the measurement range of the proposed approach. Conducting the other validation parameter is recommended, in addition to repeatability, linearity, and range, which already proceed in this research.

5. ACKNOWLEDGMENTS

This research work was funded by The Indonesia Endowment Fund for Education (Lembaga Pengelola Dana Pendidikan/LPDP), Ministry of Finance Indonesia, through the Indonesian Education scholarship scheme.

6. REFERENCES

- [1] Kothari V., Vij S., Sharma S., Gupta N., Correlation of various water quality parameters and water quality index of districts of Uttarakhand, Environmental and Sustainability Indicators, Vol. 9, No. 100093, pp. 1–8, (2021).
- [2] Wagh P., Sojan J.M., Babu S.J., Valsala R., Bhatia S., Srivastav R., Indicative Lake Water Quality Assessment Using Remote Sensing Images-Effect of COVID-19 Lockdown, Water, Vol. 13, No. 73, pp. 1–19, (2021).
- [3] Fikadu G., Determination of Selected physicochemical water quality parameters of the upper stream of Amerti watershed of Western Ethiopia, Environmental Challenges, Vol. 8, No. 100558, pp. 1–9, (2022).
- [4] Tomperi J., Isokangas A., Tuuttila T., Paavola M., Functionality of turbidity measurement under changing water quality and environmental conditions, Environmental Technology, Vol. 43, No. 7, pp. 1093–1101, (2022).
- [5] Zhang H., Zhou X., Tao Z., Lv T., Wang J., Deep learning-based turbidity compensation for ultraviolet-visible spectrum correction in monitoring water parameters, Frontiers in Environmental Science, Vol. 10, pp. 1–8, (2022).
- [6] Udoji Itodo A., Usman A., Bashir Sulaiman S., Ugbede Itodo H., Color Matching Estimation of Iron Concentrations in Branded Iron Supplements Marketed in Nigeria, Advances in Analytical Chemistry of Scientific & Academic Publishing, Vol. 2, No. 1, pp. 16–23, (2012).
- [7] Carreres-Prieto D., García J.T., Cerdán-Cartagena F., Suardiaz-Muro J., Lardín C., Implementing Early Warning Systems in WWTP. An investigation with cost-effective LED-VIS spectroscopy-based genetic algorithms, Chemosphere, Vol. 293, pp. 1–12, (2022).
- [8] Miglino D., Jomaa S., Rode M., Isgro F.,

- Manfreda S., Monitoring Water Turbidity Using Remote Sensing Techniques, in EWaS5, 2022, pages 1–5.
- [9] Viridis S.G.P., Xue W., Winijkul E., Nitivattananon V., Punpukdee P., Remote sensing of tropical riverine water quality using sentinel-2 MSI and field observations, *Ecological Indicators*, Vol. 144, No. 109472, pp. 1–17, (2022).
- [10] Guapacho J.J., Guativa J.A.V., Baquero J.E.M., Analysis of Artificial Vision Techniques for Implementation of Virtual Instrumentation System to Measure Water Turbidity, *Journal of Engineering Science and Technology Review*, Vol. 14, No. 4, pp. 161–168, (2021).
- [11] Sun B., Yang S., Yu C., Research on Multi-Parameter Portable Water Quality Detection System Based on ZYNQ Image Processing Technology, *Polish Journal of Environmental Studies*, Vol. 32, No. 2, pp. 1353–1370, (2023).
- [12] Sadar M., Making Sense of Turbidity Measurements – Advantages In Establishing Traceability Between Measurements and Technology, National Monitoring Conference, Chattanooga, TN, USA, pp. 1–10, (2004).
- [13] Buzoianu M., Practical considerations on the traceability to conventional scales, Accreditation and Quality Assurance, Vol. 5, No. 4, pp. 142–150, (2000).
- [14] Kitchener B.G.B., Wainwright J., Parsons A.J., A review of the principles of turbidity measurement, *Progress in Physical Geography*, Vol. 41, No. 5, pp. 620–642, (2017).
- [15] Supandi, Assessment correlation of total suspended solids (TSS) based on dried and sensor method, *International Journal of GEOMATE*, Vol. 19, No. 74, pp. 161–166, (2020).
- [16] Gao B., Xu Y., Lin Z., Lu M., Wang Q., Temporal and Spatial Characteristics of River Water Quality and Its Influence Factors in the TAIHU Basin Plains, Lower Yangtze River, China, *Water*, Vol. 14, No. 10, pp. 1–18, (2022).
- [17] Xiao G., Feng M., Cheng Z., Zhao M., Mao J., Mirowski L., Water quality monitoring using abnormal tail-beat frequency of crucian carp, *Ecotoxicology and Environmental Safety*, Vol. 111, pp. 185–191, (2015).
- [18] Schroeder A.B., Dobson E.T.A., Rueden C.T., Tomancak P., Jug F., Eliceiri K.W., The ImageJ ecosystem: Open-source software for image visualization, processing, and analysis, *Protein Science*, Vol. 30, No. 1, pp. 234–249, (2021).
- [19] Schindelin J., Arganda-Carreras I., Frise E., Kaynig V., Longair M., Pietzsch T., Preibisch S., Rueden C., Saalfeld S., Schmid B., Tinevez J.-Y., White D.J., Hartenstein V., Eliceiri K., Tomancak P., Cardona A., Fiji: an open-source platform for biological-image analysis, *Nature Methods*, Vol. 9, No. 7, pp. 676–682, (2012).
- [20] Świrniak G., Mroccka J., Forward and inverse analysis for particle size distribution measurements of disperse samples: A review, *Measurement*, Vol. 187, No. 110256, pp. 1–27, (2022).
- [21] Marcovina S.M., Navabi N., Allen S., Gonen A., Witztum J.L., Tsimikas S., Development and validation of an isoform-independent monoclonal antibody-based ELISA for measurement of lipoprotein(a), *Journal of Lipid Research*, Vol. 63, No. 8, pp. 1–10, (2022).
- [22] Végh R., Sörös C., Majercsik N., Sipos L., Determination of Pesticides in Bee Pollen: Validation of a Multiresidue High-Performance Liquid Chromatography-Mass Spectrometry/Mass Spectrometry Method and Testing Pollen Samples of Selected Botanical Origin, *Journal of Agricultural and Food Chemistry*, Vol. 70, No. 5, pp. 1507–1515, (2022).
- [23] APVMA, Guidelines for the validation of analytical methods for active constituent, agricultural and veterinary chemical products, No. October, pp. 1–9, (2004).
- [24] Fu Y., Hong Y., Chen L., You S., LE-GAN: Unsupervised low-light image enhancement network using attention module and identity invariant loss, *Knowledge-Based Systems*, Vol. 240, pp. 1–11, (2022).
- [25] Droujko J., Molnar P., Open-source, low-cost, in-situ turbidity sensor for river network monitoring, *Scientific Reports*, Vol. 12, No. 10341, pp. 1–13, (2022).